Archives of Materials Science and Engineering

Volume 113
Issue 2
February 2022
Pages 77-85

International Scientific Journal published monthly by the World Academy of Materials and Manufacturing Engineering

DOI: 10.5604/01.3001.0015.7017

Evaluation of stress-strain state of vehicles' metal structures elements

O. Hrevtsev [a], N. Selivanova [b], P. Popovych [c,*], L. Poberezhny [d], Yu. Rudyak [e], O. Shevchuk [c], L. Poberezhna [f], A. Ivanova [c], O. Skyba [g], O. Shashkevych [c], A. Hrytsanchuk [h]

[a] M.P. Shulgin State Road Research Institute State Enterprise, 57, Peremogy Str., Kyiv, Ukraine
[b] National Transport University, 1, M. Omelianovycha-Pavlenka Str., Kyiv, Ukraine
[c] Department of Transport and Logistics, West Ukrainian National University, 11, Lvivska str., Ternopil, Ukraine
[d] Department of Chemistry, Institute of Tourism and Geosciences, Ivano-Frankivsk National Technical University of Oil and Gas, 15, Karpatska str., Ivano-Frankivsk, Ukraine
[e] I. Horbachevsky Ternopil National Medical University, Ternopil, Ukraine
[f] Department of Ecology, Institute of Tourism and Geosciences, Ivano-Frankivsk National Technical University of Oil and Gas, 15, Karpatska str., Ivano-Frankivsk, Ukraine
[g] Faculty of Engineering of Machines, Structures and Technologies, Ternopil Ivan Pul'uj National Technical University, 56, Ruska Street, Ternopil, Ukraine
[h] Department of Petroleum Production, Institute of Petroleum Engineering, Ivano-Frankivsk National Technical University of Oil and Gas, 15, Karpatska str., Ivano-Frankivsk, Ukraine
* Corresponding e-mail address: PPopovich@ukr.net
ORCID identifier: https://orcid.org/0000-0001-6197-1060 (L.P.)

ABSTRACT

Purpose: Develop a method for determining and evaluating the stress-strain state, in particular the distribution of thermomechanical stresses in the materials of individual rotating parts of vehicles.

Design/methodology/approach: The proposed method is based on the principle of gradual approximations of the solution when the boundary conditions are satisfied on the curvilinear limiting surfaces of the disk body.

Findings: The proposed method of determining and estimating the distribution of thermomechanical stresses in the disk material makes it possible to take into account the variable geometry: thickness and presence of a hole in the central part of the disk, also correctly determine stress strain state at any point of unevenly heated rotating axial body.

Research limitations/implications: The work uses generally accepted assumptions and limitations for thermomechanical calculations.

Originality/value: It is proved that in real disks the stress-strain state is spatial, and the well-known method based on the hypotheses of the plane-stress state does not provide the possibility of calculating the values of stresses in the thickness of the disk. The obtained results can be used as a basis for improving the methodology of auto technical examination of road accidents. In addition, they can be taken into account by design engineers of car brake systems.

Keywords: Thermomechanical stresses, Disk brakes durability, Stress strain state, Vehicle reliability, Braking distance

Reference to this paper should be given in the following way:
O. Hrevtsev, N. Selivanova, P. Popovych, L. Poberezhny, Yu. Rudyak, O. Shevchuk, L. Poberezhna, A. Ivanova, O. Skyba, O. Shashkevych, A. Hrytsanchuk, Evaluation of stress-strain state of vehicles' metal structures elements, Archives of Materials Science and Engineering 113/2 (2022) 77-85. DOI: https://doi.org/10.5604/01.3001.0015.7017

METHODOLOGY OF RESEARCH, ANALYSIS AND MODELLING

1. Introduction

Based on the analysis of operating conditions of vehicles, in particular metal structures of components and parts, the dynamic loads, the temperature effect [1], and the environment were found to be the main factors that cause malfunctions and destruction of assembly units, including rotating ones (clutch mechanisms, brake discs, and other parts of their connections) [2-8].

These factors promote the formation of a scale or a film on surfaces of the specified metal structures of vehicles with consideration of surfaces' condition: a covering, roughness, hardness, etc [9-12]. The constant influence of these factors' combinations causes damage with subsequent destruction. The most characteristic types of damages are [6-8, 13-16] fatigue damage, corrosion and mechanical wear, corrosion fatigue, corrosion cracking, fretting-corrosion. Fatigue destruction of metal structures causes vehicle failure and weight loss; intensifies wear of joints; changes the value of surface roughness of parts; reduces fatigue strength [10, 17-20]. As a result, various cracks and breaks in the metal structures occur. Therefore, the reliability, efficiency, and service life of machines and their elements are reduced, the cost of repairs and elimination of damage results increases [13,21]. The service life of parts due to fatigue failure in practice is often reduced to 50%. Based on the analysis of parts' fractures, the most damageable ones are nodes and parts made of sheet steel, as well as surface of rotation, etc. [4,8,14,21,22]. Thus, during the vehicles' operation, random complex combinations of differently oriented in space force factors affect the elements of load-bearing systems due to the random nature of sources of disturbances (transport regimes, road bumps, road geometry, etc.). The research results of metal structures are significant for solving such problems: evaluation of metal structures SSS (stress-strain state) in order to define and improve the most loaded elements for the decrease in metal consumption of a design; stress distribution in the most loaded sections of the elements to predict the reliability of vehicles.

Based on the studies of disc brakes of vehicles [21,22] and the constructions designed with the help of 3D simulation technology, a thermostructural model was developed. In addition, the transitional temperature field of a car brake in certain operating conditions (hard braking, etc.) was analysed. Based on 3D simulation, the temperature curves of the brake disc in the radial and circular directions are developed, stresses and strains are computed. At the same time, the SSS of the disk is not sufficiently studied analytically, taking into account the stress level in the material. Since thermal stresses are additional and significantly affect the SSS overall level (mechanical stresses and strains) [21,22], they can cause the formation and propagation of cracks, resulting in a spontaneous destruction of metal structures [2,4,7,8,13,14,16]. Thus, to solve these problems with maximum accuracy, the provisions of the theory of elasticity should be applied, which will provide adequate simulation of stresses and displacements under operating loads. Therefore, it is advisable to improve the theoretical foundations for better understanding of thermomechanical processes in metal structures such as rotating disks of variable thickness. So, the purpose of the work is to develop a method for determining and evaluating the stress-strain state, in particular the distribution of thermomechanical stresses in the materials of individual rotating parts of vehicles.

2. Methodology

The problem of the theory of elasticity for rotating disks of variable thickness (solid with a hole in the centre of the metal structure) is known to be accurately solved with a number of assumptions and approximations [18, 21-23]. In the solution [18,23] for the rotating disk problems, the conditions for normal stresses on cylindrical surfaces are fulfilled integrally, on average, and only for a disk of small thickness.

In the proposed work, the rotating disk of variable thickness is analytically investigated taking into account the effect of uneven temperature, in contrast to [18,22,23] for the case of the solution for a flat plate.

For a solid disk of variable thickness with mass per unit volume ρ, which rotates with an angular velocity ω in the temperature field $\theta = \theta (r, z)$ bounded by symmetrical about the axis of rotation z and the axis r surfaces 22 3/2, differential equations of equilibrium in cylindrical coordinates are deduced [18,23,24]:

For replacements *u:*

$$\Delta u_1 - \frac{u_1}{r^2} + \frac{e_1}{1-2\upsilon} - 2\frac{(1+\upsilon)}{(1-2\upsilon)}\alpha\theta_1 = 0;$$
$$\Delta u_3 + \frac{e_3}{1-2\upsilon} - 2\frac{(1+\upsilon)}{(1-2\upsilon)}\alpha\theta_3 = 0; \quad (1)$$

For stresses σ:

$$\sigma_{11,1} + \sigma_{13,1} + \frac{\sigma_{11} - \sigma_{22}}{r} = 0;$$
$$\sigma_{13,1} + \sigma_{33,3} + \frac{1}{r}\sigma_{13} = 0; \quad (2)$$

In equations (1) and (2), the index after the comma means the partial derivative of the corresponding coordinate: *r*, or *z*, u_1 and u_3 – respectively, the components of radial and axial displacements; Δu_i – Laplace operator from displacements u_i $(i=1,3)$; σ_{11}, σ_{22}, σ_{33}, σ_{13} respectively components of radial, circumferential, axial and tangential stress.

Components of stresses [18,24]:

$$\sigma_{ij} = 2G\left(e_{ij} + \frac{\upsilon}{1-2\upsilon}e\delta_{ij} - \frac{1+\upsilon}{1-\upsilon}\alpha\theta\delta_{ij}\right)$$
$$i,j = 1,2,3 \quad (3)$$

If the relationship between deformation of displacements is known [18,23,24], then:

$$e_{11} = u_{1,1};$$
$$e_{22} = \frac{1}{r}u_1; \quad (4)$$
$$e_{33} = u_{3,1};$$
$$2e_{13} = u_{1,3} + u_{3,1}$$

If δ_{ij} – Kronecker symbol; α and υ – respectively, coefficients of linear thermal expansion and Poisson's ratio; $e = e_{11} + e_{22} + e_{33}$ – volumetric expansion; $G = E/2(1+\upsilon)$ – shear module; E – modulus of elasticity; A – coefficient of linear thermal expansion.

The boundary conditions on the surface of the rotating axial body under consideration are deduced [23]:

$$P_r = \sigma_{11}cos(r,n) + \sigma_{13}cos(r,n)$$
$$P_z = \sigma_{13}cos(r,n) + \sigma_{33}cos(r,n) \quad (5)$$

if *Pr* and *Pz* – projections of surface forces to directions *r* and *z; n* – normal to the surface of the body of rotation.

The proposed method is based on the principle of gradual approximations of the solution when the boundary conditions (5) are satisfied on the curvilinear limiting surfaces of the disk body.

In the first approximation the assumption is $e_{33}=u_{13}=\sigma_{33}=0$. Since, according to the condition, the cylinder is not deformed by bending, then, based on the condition $e_{33}=u_{33}=0$, the formula $u_3(r,z)=w(r)=0$ is derived. Since $\sigma_{13}=2G(u_{1,3}+u_{3,1})=0$, then $u_{1,3}=-u_{3,1}$. However, the deflection is $w(r)=0$, then

$$u_1(r,z) = u(r) \quad (6)$$

Next, based on the condition $e_{33}=0$, the value of e_{33} is found, which was previously assumed to be zero:

$$e_{33} = -\frac{\upsilon}{1-\upsilon}(e_{11} - e_{22}) + \frac{1+\upsilon}{1+\upsilon}\alpha\theta \quad (7)$$

Then, taking into account (7), we obtain for voltages σ_{11} and σ_{11}:

$$\sigma_{11} = \frac{2G}{1-\upsilon}\left[u_1 + \frac{\upsilon}{r}u - (1+\upsilon)\alpha\theta\right]$$
$$\sigma_{22} = \frac{2G}{1-\upsilon}\left[\upsilon u_1 + \frac{1}{r}u - (1+\upsilon)\alpha\theta\right] \quad (8)$$

To determine the displacement, σ_{13} is assumed not to be equal to zero. σ_{13} is determined from the first equation of system (2) taking into account formula (8) and the conditions of absence of tangential stresses on the side surfaces of the disk ($\sigma_{13}=0$ for $z=-h/2$; $z=h/2$). Then, after integration on the *z* coordinate in the range from $-h/2$ to $-h/2$ for the temperature field $\theta(r,z)=\theta_1(r)+f(z)$ [25], the formula is deduced

$$\left[\frac{1}{r}(ru)_1\right] = (1+\upsilon)\alpha\theta_{1,1} - \frac{1-\upsilon}{2G}\rho\omega^2 r \quad (9)$$

Than,

$$u(r) = \frac{1-\upsilon}{2G}\rho\omega^2\frac{r^3}{8} +$$
$$+(1+\upsilon)\alpha\frac{1}{r}\int_{a_1}^{r} r\theta_1(r)ds + \quad (10)$$
$$+A_1\frac{r}{2} + A_2\frac{1}{r}$$

if a_1 – radius of the central hole in the disk; A_2, A_1 – arbitrary constants of integration. For the case if the disk has no a hole, continuous ($a_1=0$), then A_2 should be considered equal to zero at the finiteness of displacements $u(r)$.

Further assumption is that $e_{33}\neq 0$, and $\sigma_{13}=\sigma_{33}=0$. Based on the formula (7) and taking into account (6), the displacement $u_3(r,z)$ is determined by integrating along *z* in the range from 0 to *z* :

$$u_3(r,z) = -\frac{\upsilon z}{1-\upsilon}\frac{1}{r}(ru)_1 + \frac{1+\upsilon}{1-\upsilon}\alpha\int_0^z \theta(r,z)dz \quad (11)$$

Now, based on the condition $\sigma_{13}=0$, the expression for radial displacement taking into account equations (9) and (11) is found. If $u_{1,3}=-u_{3,1}$, then after integration by *z* we obtain

$$u_1(r,z) = u(r) - \frac{z^2}{2}\left[(1-\upsilon)\alpha\theta_{1,1} + \frac{\upsilon}{2G}\rho\omega^2 r\right] \quad (12)$$

if $u(r)$ – radial displacement of the median plane points ($z = 0$). Then, based on equation (11), the value of the axial displacement $u_3(r,z)$ was deduced using expression (7), in which the sum $e_{11}+e_{22}$ is taken with consideration of the formula (12)

$$u_3(r,z) = \frac{\upsilon}{1-\upsilon}\frac{z}{r}(ru)_1 +$$
$$+\frac{\upsilon}{1-\upsilon}\frac{z^3}{6}\left[(1+\upsilon)\alpha\Delta_1\theta_1 + \frac{\upsilon}{G}\rho\omega^2\right] + \quad (13)$$
$$+\frac{1+\upsilon}{1-\upsilon}\alpha\int_0^z \theta(r,z)dz$$

if $\Delta_1\theta_1 = \theta_{1,11} + \frac{1}{r}\theta_{1,1}$

3. Results and discussion

Based on the above, the displacement $u(r)$ is a solution of equation (9), and the temperature field $\theta_1=\theta_1(r)$ is deduced from the ordinary differential equation $(\Delta_1\theta_1)_1=0$, which after integration takes the form

$$\theta_1(r) = B_1\frac{r^2}{4} + B_2 ln(r) + B_3 \tag{14}$$

if B_1, B_2, B_3 – arbitrary steels, and for this case the law of temperature distribution along the radius of the disk is considered quadratic, i.e. $B_2=0$.

Based on the found displacements, taking into account expression (14) and applying the Hooke's law, the stress is determined; and the check-up shows that σ_{13} and σ_{33} are everywhere equal to zero, and for σ_{11} and σ_{12} we obtain:

$$\begin{aligned}
\sigma_{11} &= \frac{2G}{1-v}\left\{\begin{matrix} -(1-v^2)\alpha B_1\frac{r^2}{16} - \alpha B_3 - \\ -\frac{1-v}{2G}\rho\omega^2\frac{3+v}{8}r^2 + A_1\frac{1+v}{2} - \\ -A_2\frac{1-v}{r^2} - \frac{z^2}{2}\left[\begin{matrix}\frac{(1+v)^2}{2}\alpha B_1 \\ +\frac{v(1-v)}{2G}\rho\omega^2\end{matrix}\right] \\ -(1+v)\alpha f(z)\end{matrix}\right\} \\
\sigma_{22} &= \frac{2G}{1-v}\left\{\begin{matrix} -(1-v^2)\alpha B_1\frac{3r^2}{16} - (1+v)\alpha B_3 - \\ -\frac{1-v}{2G}\rho\omega^2\frac{3+v}{8}r^2 + A_1\frac{1+v}{2} + \\ +A_2\frac{1-v}{r^2} - \frac{z^2}{2}\left[\begin{matrix}\frac{(1+v)^2}{2}\alpha B_1 \\ +\frac{v(1-v)}{2G}\rho\omega^2\end{matrix}\right] \\ -(1+v)\alpha f(z)\end{matrix}\right\} \\
\sigma_{13} &= \sigma_{33} = 0
\end{aligned} \tag{15}$$

Formulas (12), (13) and (15) are exact solutions of equilibrium equations (1) and (2), because after substitution the latter are transformed into identity.

The boundary conditions (5) are simplified due to the stresses σ_{13} and σ_{33} are equal to zero; and due to the absence of surface loads ($P_r=P_z=0$) on the curved side surface of the disk of variable thickness with a central hole, they acquire the form (Fig. 1):

$$\begin{aligned}
&\sigma_{11}=0 \text{ if } r=l(z)=l(c_i) \\
&\sigma_{11}=0 \text{ if } r=a_1, \text{ then } z=c_i \\
&(0\leq z=c_i\leq c)
\end{aligned} \tag{16}$$

if $l(z)=l(c_i)$ – equation of the profile of the side surface of the disk; a_1 – inner radius of the disk or the equation of the hole profile $a_1=const$, if $0\leq z\leq c$; c – maximum thickness of the disk; c_i – fixed value of any point of the disk body in the section parallel to the axis $0r$ and located from it by this value, and i can take all numerical values from 0 to c.

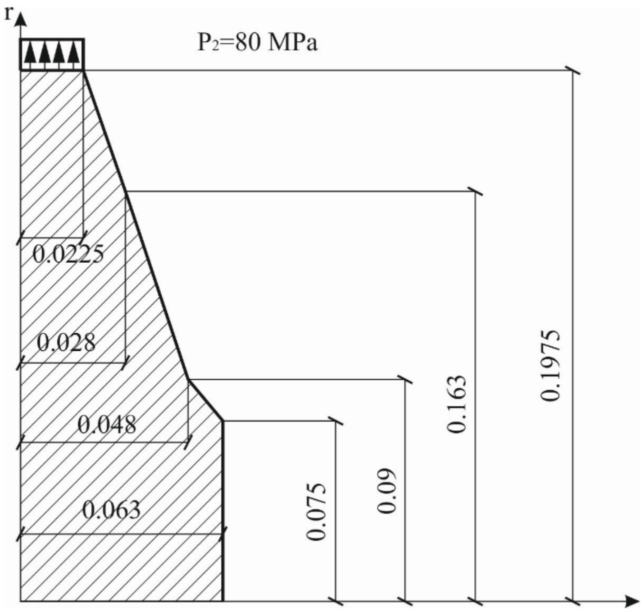

Fig. 1. Geometric dimensions of the side surface of the disk

Satisfying the boundary conditions (16) and subtracting from equations (15) the expression $(1+v)\alpha f(z)$, f – arbitrary function), the formulas for the stresses σ_{11} and σ_{22} are developed

$$\begin{aligned}
\sigma_{11} &= \frac{\alpha EB_1}{16}\left[l^2_{(z=c_i)} + a_1^2 - \frac{a_1^2 l^2_{(z=c_i)}}{r^2} - r^2\right] + \\
&+\frac{3+v}{8}\rho\omega^2\left[l^2_{(z=c_i)} + a_1^2 - \frac{a_1^2 l^2_{(z=c_i)}}{r^2} - r^2\right] \\
\sigma_{22} &= \frac{\alpha EB_1}{16}\left[l^2_{(z=c_i)} + a_1^2 - \frac{a_1^2 l^2_{(z=c_i)}}{r^2} - 3r^2\right] + \\
&+\frac{3+v}{8}\rho\omega^2\left[l^2_{(z=c_i)} + a_1^2 - \frac{a_1^2 l^2_{(z=c_i)}}{r^2} - \frac{1+3v}{3+v}r^2\right]
\end{aligned} \tag{17}$$

In addition, if the temperature field (14), which satisfies the equation of thermal conductivity, varies along the radius of a disk of variable thickness with a central hole by the quadratic law $B_2=0$ then

$$\theta_1(r) = T_1 + \frac{T_2-T_1}{a_2^2-a_1^2}(r^2-a_1^2) \tag{18}$$

if T_1 and T_2 – respectively, the temperature on the inner a_1 and outer a_2 radii of the disk, then,

$$\begin{aligned}
B_1 &= \frac{4(T_2-T_1)}{a_2^2-a_1^2} \\
B_2 &= T_1 - \frac{T_2-T_1}{a_2^2-a_1^2}a_1^2
\end{aligned} \tag{19}$$

when substituting B_1 from (19) into expressions (17), the final formulas for stresses σ_{11} and σ_{22} are deduced:

$$\sigma_{11}=\left[\frac{\alpha E}{4}\left(\frac{T_2-T_1}{a_1^2-a_1^2}\right)+\frac{3+\nu}{8}\rho\omega^2\right]+$$
$$+\left[l_{(z=c_i)}^2+a_1^2-\frac{a_1^2 l_{(z=c_i)}^2}{r^2}-r^2\right] \quad (20)$$
$$\sigma_{22}=\frac{\alpha E}{16}\left(\frac{T_2-T_1}{a_1^2-a_1^2}\right)\left[l_{(z=c_i)}^2+a_1^2-\frac{a_1^2 l_{(z=c_i)}^2}{r^2}-3r^2\right]+$$
$$+\frac{3+\nu}{8}\rho\omega^2\left[l_{(z=c_i)}^2+a_1^2-\frac{a_1^2 l_{(z=c_i)}^2}{r^2}-\frac{1+3\nu}{3+\nu}r^2\right]$$

Accordingly, for a solid disk $a_1=0$ of variable thickness, the formulas are deduced:

$$\sigma_{11}=\left[\frac{\alpha E}{4}\left(\frac{T_2-T_1}{a_2^2}\right)+\frac{3+\nu}{8}\rho\omega^2\right]+\left[l_{(z=c_i)}^2-r^2\right]$$
$$\sigma_{22}=\frac{\alpha E}{16}\left(\frac{T_2-T_1}{a_2^2-a_1^2}\right)\left[l_{(z=c_i)}^2-3r^2\right]+\frac{3+\nu}{8}\rho\omega^2\left[l_{(z=c_i)}^2-\frac{1+3\nu}{3+\nu}r^2\right] \quad (21)$$

It should be noted additionally that the profile of the disk in any case may consist of a different number of segments, both curved and rectilinear. Besides, for each section that conditionally constitutes the disk profile, the value $l_{(z=c_i)}^2$ in formulas (20) and (21) will be different.

For an example of determining the stress state by the proposed method, an unevenly heated (temperature distribution law along the radius of the disk is square) solid rotating disk of variable thickness is under study, its quarter (due to axial symmetry) is shown in Figure 2. Determination of stresses in a given disk by the method of successive approximations (Kinasoshvili method) in a flat formulation of the problem solution is concerned in [26].

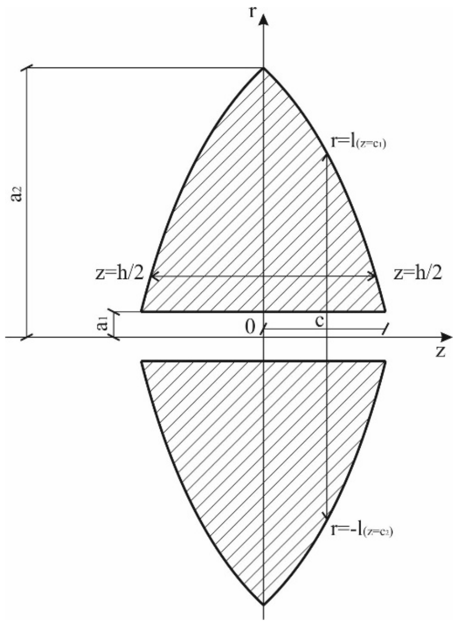

Fig. 2. Cross section of a disk of variable thickness

The disk under study rotates with a constant angular velocity ω = 847.8 *rad/s* and is exposed to a load P_r evenly distributed on the outer surface of the disk rim with an intensity 80.0 *MPa*. The density of the disk material is $\rho=0.8\cdot 10^4$ kg/m^3. Poisson's ratio is ν = 0.3. The value of the modulus of elasticity E and the coefficient of linear thermal expansion α for points on different radii of the disk are taken from the [27-30]. For the convenience of comparing the results of the calculation by both methods, the stresses σ_{11} and σ_{22} were determined at the same horizontal sections of the disk body. The values of stresses σ_{11} and σ_{22} found by the proposed method, are written in Table 1 and Table 2. The Tables show that the value of radial stresses σ_{11} (Tab. 1) decreases, depending on the change in thickness, in the direction from the axis $0r$ to the edge of the disk and from the axis 0z to the rim of the disk. As for the values σ_{22} (Tab. 2), due to uneven heating and deformation in the material of the disk, in addition to tensile stresses, the compressive stresses occur. The transition from tension to compression in the body of the disk is as follows: in the radial direction from the axis of rotation $0z$ to the rim and in the horizontal direction from the axis $0r$ to its side surface. To compare the stresses σ_{11} and σ_{22} determined by two methods, the graphical dependencies are shown in Figure 3. Moreover, the dotted lines show the plots $\sigma_{11.s.a}$ and $\sigma_{22.s.a}$, found by the method of successive approximations *(s.a)*, and the solids show the plots developed by the average value *(a.v)* of the stresses $\sigma_{11.a.v}$ and $\sigma_{22.a.v}$, which are considered in horizontal sections on the radii of the disk under study. In work [31] presents the distribution of the constraint equivalent of Von Mises.

Calculations of thermomechanical stresses based on the simulation results established their maximum values, which differ from the mechanical stresses calculated for similar initial conditions. As in [31], there are limitations at the level of the disk bowl, taking into account the design features, possible further destruction at the level of the disk bowl.

Based on the comparison of the above plots, the values of radial stresses deduced by applying the developed method are found to be smaller (approximately 11%) than the values $\sigma_{11.s.a}$ which are obtained by the method of successive approximations. Besides, the largest differences (22%) occur between $\sigma_{22.a.v}$ and $\sigma_{11.a.v}$.(Fig. 3). They are observed in those sections of the disk body where there are compressive circular stresses.

Such differences indicate the spatial stress-strain state in real disks; the classical method of successive approximations is known to be based on the hypotheses of the plane-stress state. Therefore, the values of stresses σ_{11} and σ_{22} with consideration of the disk thickness cannot be defined by applying the classical method.

Table 1.
Calculated values of radial stresses

r_M \ z_M	0.0000	0.0050	0.0100	0.0150	0.0225	0.0257	0.0295	0.0350	0.0405	0.0459	0.0550	0.0605	0.0630
0.1975	80.0	80.0	80.0	80.0	80.0								
0.1775	168.1	168.1	168.1	168.1	168.1	0							
0.1575	256.7	256.7	256.7	256.7	256.7	83.4	0						
0.1375	335.3	335.3	335.3	335.3	335.3	160.1	74.9	0					
0.1175	402.9	402.9	402.9	402.9	402.9	226.8	140.9	58.4	0				
0.0975	459.4	459.4	459.4	459.4	459.4	283.0	196.8	120.7	54.9	0			
0.0775	504.4	504.4	504.4	504.4	504.4	328.0	241.8	165.7	99.9	45.4	11.3	0	
0.0575	539.9	539.9	539.9	539.9	539.9	363.3	277.0	200.7	134.9	80.3	46.1	34.8	29.9
0.0375	564.0	564.0	564.0	564.0	564.0	387.4	301.2	225.0	159.2	104.6	70.5	59.2	54.3
0.0175	577.8	577.8	577.8	577.8	577.8	401.3	315.1	239.0	173.3	118.7	84.6	73.3	68.4
0.0000	582.1	582.1	582.1	582.1	582.1	405.6	319.4	243.2	177.4	122.8	88.7	77.4	72.4

Table 2.
Calculated values of circumferential stresses

r_M \ z_M	0.0000	0.0050	0.0100	0.0150	0.0225	0.0257	0.0295	0.0350	0.0405	0.0459	0.0550	0.0605	0.0630
0.1975	-529.1	-529.1	-529.1	-529.1	-529.1								
0.1775	-397.7	-397.7	-397.7	-397.7	-397.7	-559.4							
0.1575	-218.0	-218.0	-218.0	-218.0	-218.0	-391.4	-474.7						
0.1375	-36.4	-36.4	-36.4	-36.4	-36.4	-211.6	-292.5	-371.7					
0.1175	128.4	128.4	128.4	128.4	128.4	-47.7	-133.5	-29.4	-274.5				
0.0975	269.5	269.5	269.5	269.5	269.5	93.0	6.8	-69.3	-135.0	-190.0			
0.0775	384.4	384.4	384.4	384.4	384.4	207.9	121.8	45.6	-2.1	-74.6	-108.7	-120.0	
0.0575	473.6	473.6	473.6	473.6	473.6	297.0	210.7	134.4	68.6	14.0	-20.1	-31.5	-36.4
0.0375	535.5	535.5	535.5	535.5	535.5	359.3	273.0	196.8	131.0	76.5	42.4	31.0	26.1
0.0175	571.6	571.6	571.6	571.6	571.6	395.1	38.9	232.8	167.1	112.5	78.4	67.1	62.2
0.0000	582.1	582.1	582.1	582.1	582.1	405.6	319.4	243.2	177.4	122.8	88.7	77.4	72.4

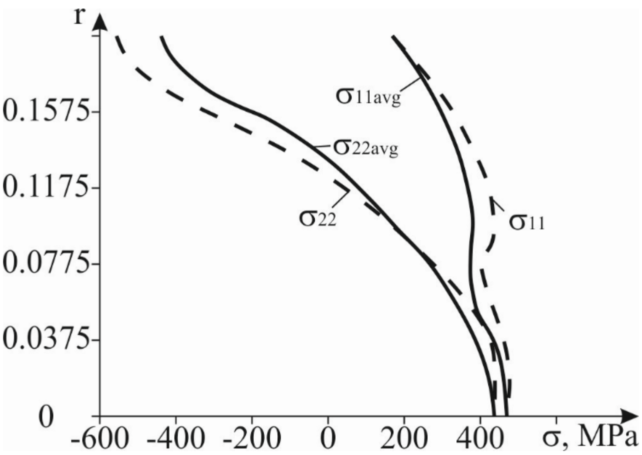

Fig. 3. Graphical dependences of stresses on the radial coordinate

In addition, in this case, the condition of equality of stresses σ_{11} and σ_{22} on the axis of rotation $0z$ in the calculations by the method of successive approximations is not fulfilled, i.e. if $r = 0$, then the stress $\sigma_{11.s.a}$ should be equal to the stress $\sigma_{22.s.a}$, but we have $\sigma_{11.s.a}=\sigma_{11.s.a}$ with $r = 0.0175$ m.

Therefore, the proposed method for estimating the stress-strain state of the metal structures' elements of vehicles can be effectively applied in the SSS simulation of individual parts of vehicles. This method of determining and estimating the distribution of thermomechanical stresses in the disk material makes it possible to take into account the variable geometry, in particular the thickness and the presence of a hole in the central part of the disk; to determine correctly the SSS at any point of unevenly heated rotating axial body.

Buses operating on urban public transport routes have a re-short-term mode of braking with a significant number of brakes relatively small efficiency. The ratio of the total braking distance to the length of the route reaches 7%. Average the value of decelerations is 1.32-1.43 m/s^2, and the number of emergency braking (with deceleration more than 3 m/s^2) does not exceed 1% of the total number of brakes. A significant number of brakes that account for 1 km of the road, leads to heating of the brake mechanisms (their temperature gradually increases and by the end of the turn on the route stabilizes at 260-280 °C). At such temperatures there is a sharp decrease in the coefficient of friction, and, accordingly, the braking torque and efficiency braking.

Theoretical [31] and landfill studies [32-34] have shown that the temperature of the brakes affects the length of the braking distance, and this effect is quite noticeable (increase by 3-4 m). From the analysis of relative differences between the lengths of braking distance for cold and hot brakes (compared to cold brakes) at the same initial speed, it was found that it decreases with increasing speed (relative difference at 40 km/h – 28%, and at 60 km/h – 15%).

This can be explained by the fact that the buses are equipped with ABS, and during emergency braking the wheels are not locked. That is, the brake mechanisms heat up and lose their effectiveness during emergency braking. Since the length of the braking distance for a larger initial speed is greater, the brakes are heated to a higher temperature. That is, the effect of brake temperature on the braking distance is greater than the lower initial speed. It should be borne in mind that public transport in cities moves at an average technical speed in the range of 30-50 km/h. The obtained results can be used as a basis for improving the methodology of auto technical examination of road accidents. In addition, they can be taken into account by bus drivers on urban routes when choosing a safe distance in heavy traffic, as well as design engineers of car brake systems.

4. Conclusions

On the basis of theoretical researches, the methods of determining and evaluating the stress-strain state, in particular the distribution of thermomechanical stresses in the materials of cylindrical rotating parts of vehicles is developed.

The implementation of the proposed mathematical model is demonstrated on the problem of determining the radial stresses in the body of a disk of variable thickness rotating with angular velocity and subjected to a uniformly distributed load on the surface. It is proved that in real disks the stress-strain state is spatial, and the well-known method based on the hypotheses of the plane-stress state does not provide the possibility of calculating the values of stresses in the thickness of the disk.

References

[1] S. Zhu, C. Cai, Interface damage and its effect on vibrations of slab track under temperature and vehicle dynamic loads, International Journal of Non-Linear Mechanics 58 (2014) 222-232. DOI: https://doi.org/10.1016/j.ijnonlinmec.2013.10.004

[2] Ya. Doroshenko, V. Zapukhliak, Ya. Grudz, L. Poberezhny, A. Hrytsanchuk, P. Popovych, O. Shevchuk, Numerical simulation of the stress state of an erosion-worn tee of the main gas pipeline, Archives of Materials Science and Engineering 101/2 (2020) 63-78. DOI: https://doi.org/10.5604/01.3001.0014.1192

[3] P.V. Popovych, O.L. Lyashuk, O.S. Shevchuk, O.P. Tson, L.Ya. Poberezhna, I.M. Bortnyk, Influence of organic operation environment on corrosion properties of metal structure materials of vehicles, INMATEH – Agricultural Engineering 52/2 (2017) 113-118.

[4] P.V. Popovych, O.L. Lyashuk, I.S. Murovanyi, V.O. Dzyura, O.S. Shevchuk, V.D. Myndyuk, The service life evaluation of fertilizer spreaders undercarriages, INMATEH – Agricultural Engineering 50/3 (2016) 39-46.

[5] I.V. Lytvynenko, P.O. Maruschak, S.A. Lupenko, P.V. Popovych, Modeling of the Ordered Surface Topography of Statically Deformed Aluminum Alloy, Materials Science 52 (2016) 113-122. DOI: https://doi.org/10.1007/s11003-016-9933-1

[6] R.A. Barna, P.V. Popovych, Influence of operating media on the fatigue fracture of steels for elements of agricultural machines, Materials Science 50/3 (2014) 377-380. DOI: https://doi.org/10.1007/s11003-014-9729-0

[7] B.M. Hewko, P.V. Popovich, A.Y. Diachun, O.L. Lyashuk, R.O. Liubachivskyi, The study of bulk material kinematics in a screw conveyor-mixer, INMATEH – Agricultural Engineering 47/3 (2015) 156-163.

[8] P. Popovych, L. Poberezhny, O. Shevchuk, I. Murovanyi, T. Dovbush, Yu. Koval, H. Hrytsuliak, Evaluation of strength of carrying metal structures of trailers, Journal of Achievements in Materials and Manufacturing Engineering 100/2 (2020) 58-69. DOI: https://doi.org/10.5604/01.3001.0014.3345

[9] J.C. Brown, A.J. Robertson, S.T. Serpento, Motor vehicle structures: concepts and fundamentals, Butterworth-Heinemann, Oxford, UK, 2001.

[10] G. Vaičiūnas, G. Bureika, S. Steišūnas, Research on metal fatigue of rail vehicle wheel considering the wear intensity of rolling surface, Eksploatacja i Niezawodność – Maintenance and Reliability 20/1 (2018) 24-29. DOI: http://dx.doi.org/10.17531/ein.2018.1.4

[11] F. Zhu, D. Persson, D. Thierry, Formation of corrosion products on open and confined metal surfaces exposed to periodic wet/dry conditions – a comparison between zinc and electrogalvanized steel, Corrosion 57/7 (2001) 582-590. DOI: https://doi.org/10.5006/1.3290385

[12] G.S. Cole, A.M. Sherman, Light weight materials for automotive applications, Materials Characterization 35/1 (1995) 3-9. DOI: https://doi.org/10.1016/1044-5803(95)00063-1

[13] P. Popovych, O. Shevchuk, V. Dzyura, L. Poberezhna, V. Dozorskyy, A. Hrytsanchuk, Assessment of the influence of corrosive aggressive cargo transportation on vehicle reliability, International Journal of Engineering Research in Africa 38 (2018) 17-25. DOI: https://doi.org/10.4028/www.scientific.net/JERA.38.17

[14] P.V. Popovych, V. Dzyura, O.S. Shevchuk, Reliability estimation of transport means elements under the action of cyclic loads and corrosive environment, International Journal of Automotive and Mechanical Engineering 15/4 (2018) 5793-5802. DOI: https://doi.org/10.15282/ijame.15.4.2018.6.0443

[15] B. Sokil, O. Lyashuk, M. Sokil, P. Popovich, Y. Vovk, O. Perenchuk, Dynamic Effect of Cushion Part of Wheeled Vehicles on Their Steerability, International Journal of Automotive and Mechanical Engineering 15/1 (2018) 4880-4892. DOI: https://doi.org/10.15282/ijame.15.1.2018.1.0380

[16] P. Popovych, L. Poberezhny, O. Shevchuk, I. Murovanyi, L. Poberezhna, A. Hrytsanchuk, Y. Koval, Corrosion-fatigue failure of tractor trailers metal materials in aggressive environments, Koroze a Ochrana Materialu 64/2 (2020) 45-51. DOI: https://doi.org/10.2478/kom-2020-0007

[17] J.R. Davis (Ed.), Surface engineering for corrosion and wear resistance, ASM international, Materials Park, OH, United States, 2001.

[18] L. Poberezhny, P. Maruschak, A. Hrytsanchuk, B. Mischuk, D. Draganovska, L. Poberezhna, Impact of AC current density on material corrosion of distribution pipelines, Koroze a Ochrana Materialu 61/5 (2017) 178-184. DOI: https://doi.org/10.1515/kom-2017-0023

[19] S. Kubo, H. Tsuchiya, J. Ikeuchi, Wear properties of metal/carbon composite pantograph sliders for conventional electric vehicles, Quarterly Report of RTRI 38/1 (1997) 25-30.

[20] M. Senthil Kumar, S. Vijayarangan, Analytical and experimental studies on fatigue life prediction of steel and composite multi-leaf spring for light passenger vehicles using life data analysis, Materials Science (Medžiagotyra) 13/2 (2007) 141-146.

[21] Q. Jian, Y. Shui, Numerical and experimental analysis of transient temperature field of ventilated disc brake under the condition of hard braking, International Journal of Thermal Sciences 122 (2017) 115-123. DOI: https://doi.org/10.1016/j.ijthermalsci.2017.08.013

[22] A. Belhocine, M. Bouchetara, Thermomechanical modelling of dry contacts in automotive disc brake, International Journal of Thermal Sciences 60 (2012) 161-170. DOI: https://doi.org/10.1016/j.ijthermalsci.2012.05.006

[23] L.Y. Pobereznyi, L.Y. Poberezhna, P.O. Maruschak, S.V. Panin, Assessment of potential environmental risks from saline soils subsidence, IOP Conference Series: Earth and Environmental Science 50/1 (2017) 012046. DOI: https://doi.org/10.1088/1755-1315/50/1/012046

[24] M.H. Sadd, Elasticity: theory, applications, and numerics, Second Edition, Academic Press, 2009.

[25] A.S. Saada, Elasticity: theory and applications, Elsevier, 2013.

[26] A.I. Lurie, Non-linear theory of elasticity, Elsevier, 2012.

[27] E. Melan, H. Parkus, Thermal stresses caused by stationary temperature fields, Springer-Verlag, Vienna, 1953.

[28] A.F. Riabov, Yu.M. Fedorenko, On one method for solving the problem of the theory of thermoelasticity for bodies of revolution, Mathematical Methods and Physicomechanical Fields 28 (1988) 58-62.

[29] E. Logan Jr, Handbook of turbomachinery, CRC Press, 2003.

[30] N.N. Malinin, Prochnost' turbomashin, Mashgiz, 1962 (in Russian).

[31] A. Belhocine, M. Bouchetara, Temperature and thermal stresses of vehicles gray cast brake, Journal of Applied Research and Technology 11/5 (2013) 674-682. DOI: https://doi.org/10.1016/S1665-6423(13)71575-X

[32] S.F. Iombriller, A.C. Canale, Analysis of emergency braking performance with particular consideration of temperature effects on brakes, Journal of the Brazilian Society of Mechanical Sciences 23/1 (2001) 79-90. DOI: https://doi.org/10.1590/S0100-73862001000100007

[33] Ye.Yu. Fornalchyk, I.A. Mohyla, O.S. Mikhotskyy, Otsinyuvannya vplyvu temperatury hal′m na dovzhynu hal′mivnoho shlyakhu, Avtoshlyakhovyk Ukrayiny 2 (2013) 2-5 (in Ukrainian).
[34] A. Erd, M. Jaśkiewicz, G. Koralewski, D. Rutkowski, J. Stokłosa, Experimental research of effectiveness of brakes in passenger cars under selected conditions, Proceedings of the 2018 XI International Science-Technical Conference Automotive Safety, Žastá, Slovakia, 2018, 1-5.